Finite Element Analysis of Origami-Based Sheet Metal Folding Process

Muhammad Ali Ablat
Department of Mechanical Engineering,
University of California, Merced,
Merced, CA 95343
e-mail: amaimaitiaili@ucmerced.edu

Ala Qattawi[1]
Department of Mechanical Engineering,
University of California, Merced,
Merced, CA 95343
e-mail: aqattawi@ucmerced.edu

Origami-based sheet metal (OSM) folding is a novel approach regarded as extension of the origami technique to sheet metal. It requires creating numerous features along the bend line, called material discontinuities (MD). Material discontinuities control the material deformation and result in reduced bending force (BF), minimal tooling, and machinery requirements. Despite the promising potential of OSM, there is little understating of the effect of the selected MD shape and geometry on the final workpiece. Specifically, this is of interest when comparing the manufacturing energy and cost allocations for OSM with a well-establish process for sheet metal such as stamping. In this work, wiping die bending of aluminum sheet with different MD shapes and geometries along the bend line is investigated using finite element analysis (FEA) and compared to traditional sheet bending in terms of stress distribution along the bending line, required bending force and springback. The FEA results are validated by comparing it to the available empirical models in terms of bending forces. This study found that OSM technique reduced the required bending force significantly, which has important significance in energy and cost reduction. The study also found each MD resulted with different bending force and localized stress. Hence, MD are ranked in terms of the required force to bend the same sheet metal type and thickness for further future investigation. Springback is decreased due to application of MD. Meanwhile, MD generated localized high stress regions along the bending line, which may affect load-bearing capability of the final part. [DOI: 10.1115/1.4039505]

Keywords: sheet metal bending, origami folding, material discontinuities, finite element, bending force

Introduction

Sheet metal bending is one of the main approaches to fabricate three-dimensional (3D) parts and it is widely used in mass production. However, conventional manufacturing process like stamping generally requires high tooling cost for the die design and manufacturing, which are shape dedicated to specific final parts. During the bending process, sheet metal experiences large elastic–plastic deformation and design of final part requires consideration for the effect of springback and accurate planning for machinery displacement, such as the punch–die displacement to locate the bending line correctly. Studies have been conducted to reduce the springback and increase bending accuracy of sheet metal. However, springback remains to be one of the major problems in sheet metal fabrication [1–4].

The practical example of an actual sheet metal part produced by origami-based sheet metal (OSM) technique shows a minimal springback effect and high accuracy in locating bending line. It also shows a potential in tooling reduction [5–7]. Figure 1 shows a design of a floor panel fabricated by OSM, the 3D geometry was folded using a single two-dimensional flat pattern. The folding process required minimal tooling and mostly done manually. However, the design requirements of sheet metal impose more restrictions to the folding procedures that are conventionally followed in paper origami. When handling sheet metal folding the problem is described as a rigid origami concept. The faces or sides of the 3D part are not deformed nor bent. All folding and material deformation is localized along the bend or creases. Researchers tackled the rigid origami application by introducing two layers of materials in a 3D part to accommodate rigidity and flexibility requirements of the folding line [8–11]. However, in this manuscript, the focus is one layer material for the 3D part while introducing flexibility along bend line by degrading the material with material discontinuities (MD).

Origami-based sheet metal technique utilizes MD in folding process. Material discontinuities are fabricated by removal of material completely or partially through thickness direction of sheet metal along the bend line. It can be fabricated using laser

Fig. 1 An example of floor panel of aluminum sheet produced with OSM technique, shown part was folded manually from a single flat pattern with minimal tooling [12,13]

[1]Corresponding author.

Contributed by the Materials Division of ASME for publication in the JOURNAL OF ENGINEERING MATERIALS AND TECHNOLOGY. Manuscript received September 15, 2017; final manuscript received January 19, 2018; published online April 6, 2018. Assoc. Editor: Huiling Duan.

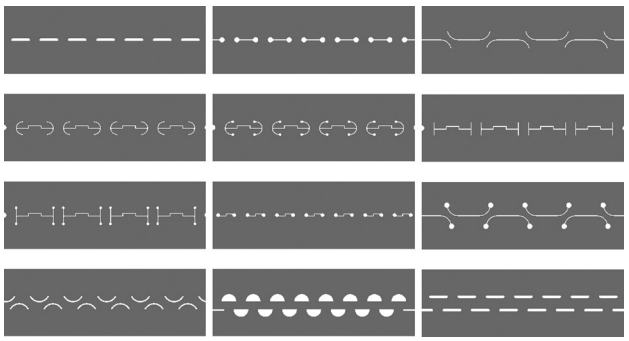

Fig. 2 Various possible MD designs for OSM technique. Either laser cutting or stamping processes can be used to create them.

cutting process or progressive stamping. Material discontinuities can also be created by stamping where no material removal is present. Stamping creates a deformed pattern along the bend line to guide the folding.

Material Discontinuities

Researchers suggested different shapes and geometries for the MD [14,15] and some of the MD features have been already commercialized as well. Figure 2 illustrates possible MD features to be created along the bend line of the OSM parts. In most cases, if not all, the MD are arranged symmetrically along the bend line. Alternatively, MD appears in symmetric pairs on the two sides of a bending line. The removal of material from the sheet metal or deformed pattern in the stamped MD can substantially affect strength and functional performance of the final products. By applying MD on the sheet metal, it is expected that the MD will serve as locaters for the predefined bending line and thus help achieve high dimension accuracy with minimal design analysis in terms of locating the bend line. In addition, different arrangements of MD can influence the mechanical load-bearing capabilities and its two-dimensional flat pattern.

In OSM technique, the MD can increase the accuracy of bending line location and increase process efficiency by reducing cost and energy. However, the current state of the art for the technique lacks the information to quantify the advantage of the OSM over the traditional manufacturing process of sheet metal, especially for mass production. For example, study [16] showed that to stamp 1 kg of steel, the energy spent in manufacturing process only can range from 5.1 to 9.69 MJ/kg due to the high tonnage presses involved and the energy lost in pressing machines. Therefore, the purpose of this study is to investigate the effect of several MD on the sheet metal bending process.

The presented study is extension of previous study [17] and attempts to rank and evaluate the MD suggested shapes affecting the bending force (BF), stress concentration and resulted springbuck. Further analysis is needed in future to correlate the MD geometry and dimensions with the optimized bending line design, (i.e., the acceptable dimensions of the MD and the alternating distance between the serial MD along the bending line). In addition, further investigation is necessary to elaborate the effect of the MD on the final mechanical proprieties of the 3D folded parts.

In this work, four different types of MD are chosen for study. All four are produced by laser cutting. The name convention is as follows: The chosen MD are named as MD-14, MD-33, MD-243, and MD-443, also illustrated in Fig. 3. As can be seen in Fig. 3, in this study, two rules govern the arrangement of the MD along the bending line. One is that only one pairs of MD is arranged with respect to bend line. MD-14 and MD-33 are examples that MD lie along the bend line. While, MD-243 and MD-433 are examples of positioning MD at the two sides of bend line. The second rule is

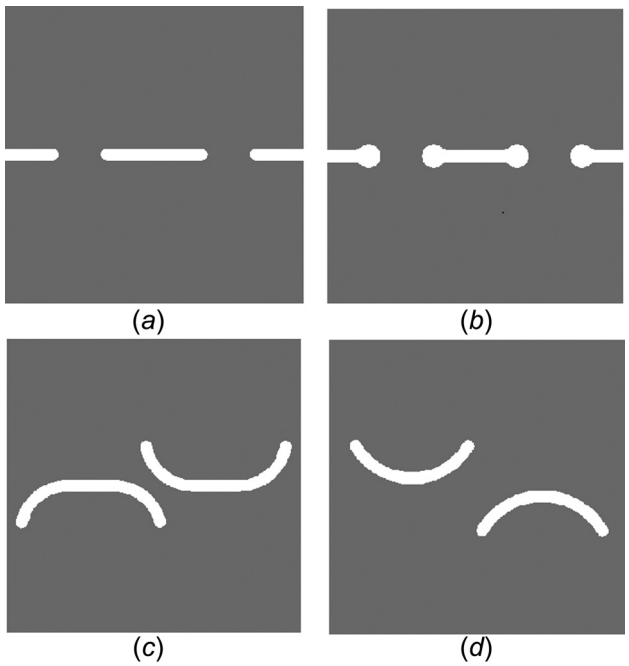

Fig. 3 The selected MD shapes for the FEA study presented in this work, the assigned number for each shape is for distinguishing purpose. All of the MD are laser cut and the same length of material is left along bend line after removal of material for comparison purpose: (*a*) MD-14, (*b*) MD-33, (*c*) MD-243, and (*d*) MD-433.

regarding the percentage of removed material. In order to be able to make comparison between cases, the dimensions of MD are designed such that there are identical lengths of material left along the bending line after laser cutting. In case these two rules conflict, rule one prevails.

Finite Element Analysis of Sheet Metal Bending

Finite element method (FEM) has become one of the main methods for studying sheet metal bending along with experiment and theoretical research. Early works studied sheet metal forming using FEM dates back to pioneer works by Wifi [18], Gotoh and Ishisé [19], and Wang and Budiansky [20] in late 1970s. Over the past decades, with the development of simulation strategies and specific purpose simulation software, now finite element analysis (FEA) of sheet metal bending is able to provide results with sufficient accuracy [21]. Reported work [4,22–28] discussed different solution methods in simulation of sheet metal forming. Makinouchi et al. [27] classified formulation into three main categories, which are dynamic explicit, static explicit, and static implicit formulation. Further, solution strategies were categorized into three, which are incremental method, large step method, and one-step method. Thus, in FEM codes, the various FEM formulations are combined with different solution strategies. In summary, one can classify solution methods into five different categories; they are static explicit method, dynamic explicit method, static implicit incremental method, static implicit large step method, and static implicit one-step method. These methods are compared with one another in the work of Oniate et al. [29] and Yang et al. [30], respectively.

Finite Element Simulation

In this study, 3D wiping die bending of aluminum 2036-T4 sheet is simulated for different cases using commercial FE software ANSYS version 17.2. Schematic of wiping die bending is shown in Fig. 4.

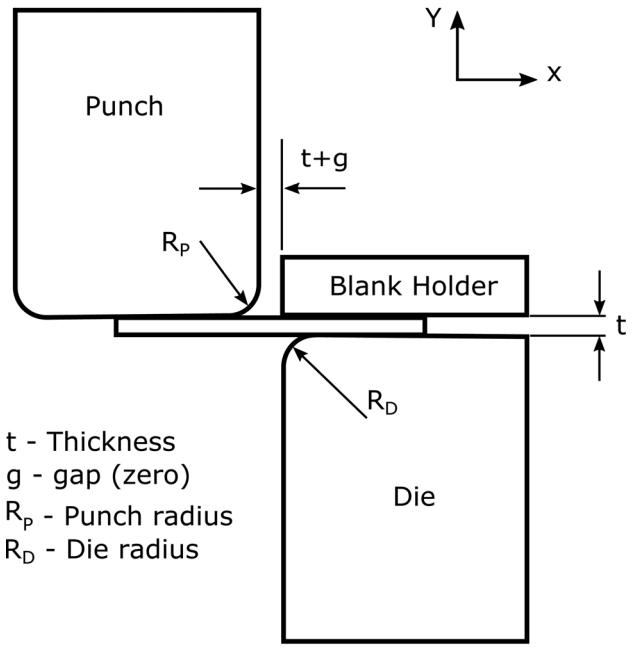

Fig. 4 Wiping die bending configuration

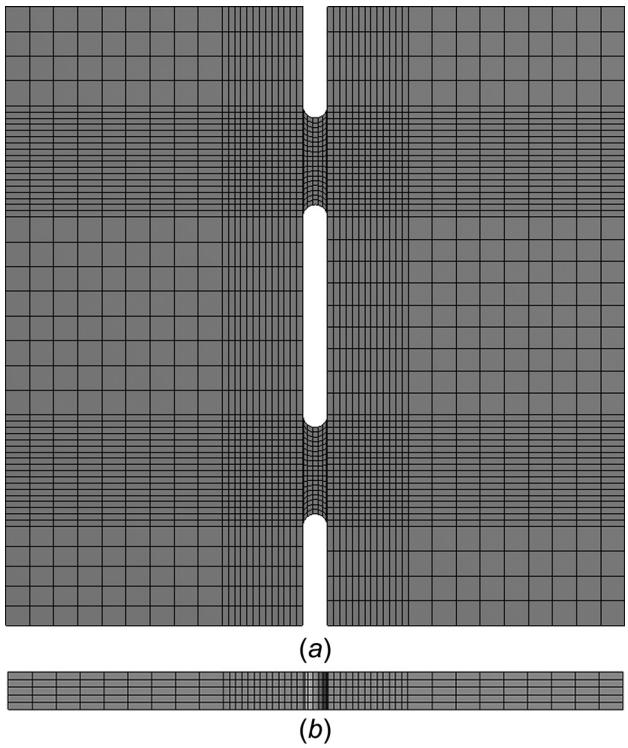

Fig. 5 Meshing illustration: (*a*) meshing of MD-14, top view and (*b*) MD-14 five mesh layers in thickness direction

In wiping die bending, the basic operation is to deform sheet under downward movement of a punch into 90 deg. Sheet is clamped between a die and a blank-holder. The sheet is rectangular in shape having 50 mm in length, 50 mm in width, and 3 mm in depth. The radius of die (R_D) and the radius of punch (R_P) are both set to 3 mm. Punch dimensions are 50 mm (width) × 50 mm (height) × 30 mm (length). Die dimensions are 50 mm (width) × 50 mm (height) × 40 mm (length). Blank holder has dimensions of 50 mm (width) × 10 mm (height) × 40 mm (length). The aluminum sheet 2036-T4 has an ultimate tensile strength of 338 MPa, a yield strength value of 193 MPa, a strength coefficient of 598 MPa, and a strain hardening exponent of 0.216.

In the simulation process, the sheet is set to elastic–plastic with isotropic hardening since it experiences large deformation during the bending process. Die is fixed throughout the simulation. Blank holder is set to be free only in the *Y* degree-of-freedom. Displacement of the sheet in *Z*-axis is restricted due to symmetry condition. There are four steps in simulation. First, a ramped load with maximum value of 2×10^5 N is applied on top of the blank holder to hold sheet firmly during bending. In the second step, 25 mm of displacement in the negative *Y* direction is imposed on punch. By the end of the second step, bending will be completed. Third and fourth steps are to unload the sheet by separating punch from sheet and unloading blank holder so that springback can be evaluated.

In order to achieve accurate results, five layers of element 20-node hexa elements are generated along the thickness direction of sheet [31]. This would result in ten integration point along the thickness of sheet. Punch, blank holder, and die are simulated as rigid bodies and linear four-node quadrilateral elements are used for them. The number of elements is kept constant for each of the die, punch, and blank holder in all cases. Mesh of the sheet is dominantly made of 20-node hexahedron elements, but prism elements are also generated around MD. A refinement is made along with the bending line. A typical meshing of sheet is illustrated in Fig. 5.

The friction coefficient of 0.12 is considered in these simulations. There are three frictional surface-to-surface contact pairs between sheet and rigid parts (punch, die, and blank holder). Augmented Lagrangian formulation is used for contact simulation. The objective of these cases is to compare regular sheet that has no MD and sheet with MD in terms of bending force required to bend sheet metal, maximum stress caused during the bending and springback angle. It will serve as an indication of the effect of bending force reduction in the case of OSM, which will result in reduction in the necessary manufacturing energy. In addition, the comparison between the different shapes of MD can assist in designing OSM parts with optimized bending force requirements and stresses generated along the bend line. Hence, there are four cases where sheets with the chosen MD are simulated while the last one is a regular sheet without any MD.

Finite Element Simulation Process and Results Discussion

Overall, simulation process went well except convergence problem. Obtaining full convergence of simulation especially in the bending process (which is second step in simulation) became problematic. The reason was diagnosed to be applying punch displacement boundary condition too fast and so elements became highly distorted.

It was overcome by increasing number of time steps, i.e., slower application of loads. Number of time steps required for convergence at the bending process varied over different MD. Regular sheet and MD-433 required 200 time steps while MD-14, MD-33, and MD-243, needs 250 time steps. These time steps are uniformly applied during the bending process.

Mesh Convergence Study

In order to achieve accurate results from the simulation, mesh convergence studies have been conducted. Each MD case is simulated with finer mesh size along the bending line of sheet until mesh convergence is obtained. Then variation of maximum Von Mises stress is evaluated over mesh sizes. Figure 6 shows the results of mesh convergence studies.

Required Bending Force

Bending force is evaluated for all cases over the punch displacement. Figure 7 shows that in all studied cases, the bending

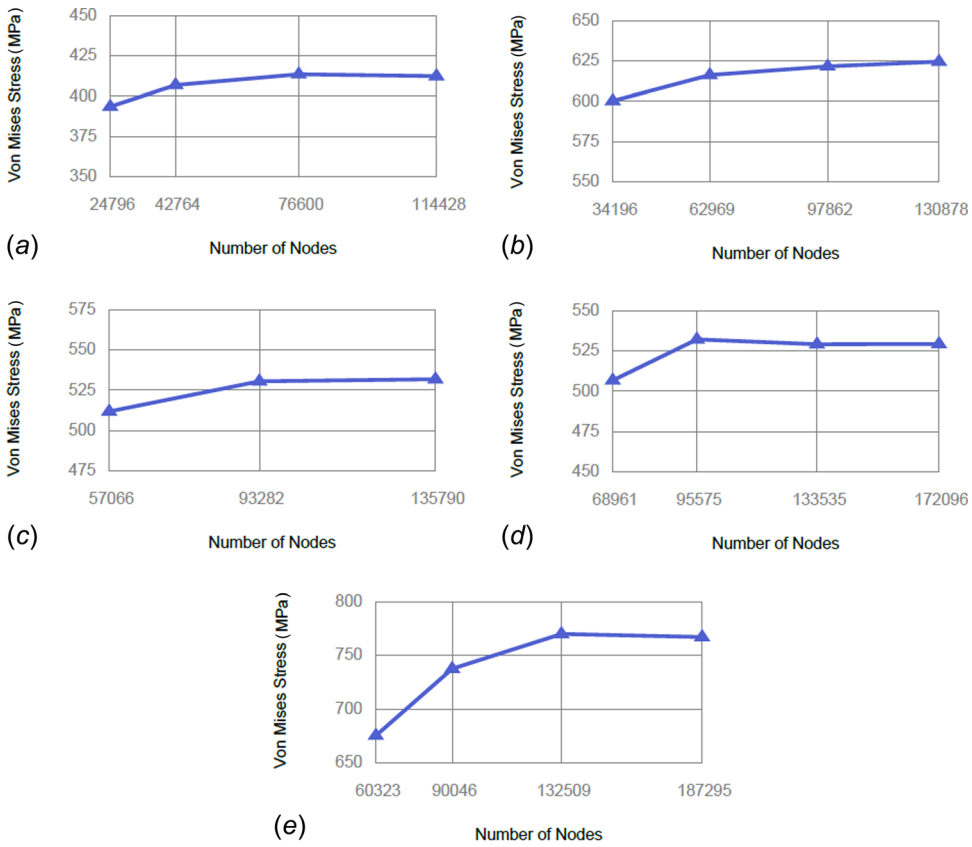

Fig. 6 Mesh convergence studies result: (*a*) without MD, (*b*) MD-14, (*c*) MD-33, (*d*) MD-243, and (*e*) MD-433

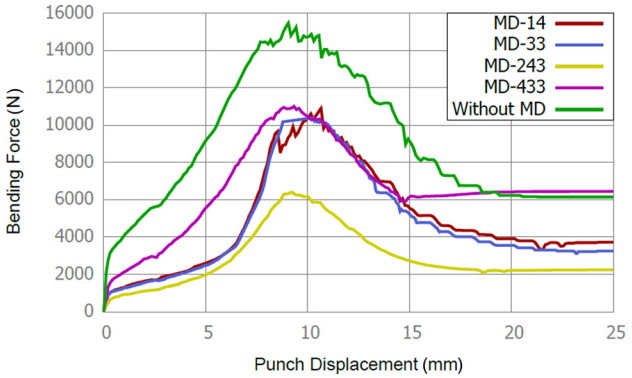

Fig. 7 Bending force versus punch displacement plot for each of the studied MD cases and the traditional sheet metal case with no MD along the bend line

force over the punch displacement has a similar pattern. It increased to a maximum value and then decreased followed by a rather steady value to the end of punch displacement. As expected, bending force required for sheets with MD reduced substantially compared to the sheet that has no MD. The reduction of the magnitude of the required bending force varies depending on the type of MD, see Table 1. The reduction reached as high as 59% in the case of MD-243, which is the maximum reduction, and it is 29% in the case of MD-433, which is the least reduction among the four cases. The reduction implies the possibility of performing bending operation with light tools even by hand for some sheet metal thicknesses. Physically, the reduction in the required bending force is a result of the removing materials along the bend line that resist to punch movement and thus there are less resisting force to bending.

Table 1 BF evaluation

Cases	Simulated BF (N)	Empirical BF (N)	Reduction in BF compared to no MD (%)
MD-243	6398	—	59
MD-33	10,362	—	33
MD-14	10,900	—	29.5
MD-433	11,012	—	29
Without MD	15,459	15,210	—

In the case without MD, the bending force-punch displacement curve displayed a series of fluctuation after reaching the maximum bending force value. This phenomenon is caused by the deformed material flow that has been accumulated within the gap between punch and die. As the punch goes down, the sheet experiences more deformation and as a result deformed material flows to the gap between the punch and the die. As more material accumulates in the gap, it increases the resistance to the punch movement and the resistance caused fluctuation of bending force.

Empirical Evaluation of Bending Force

The simulation results, for this phase of the research, are validated through empirical formula that predicts the maximum bending force for a wiping die. Maximum bending force for a wiping die is given in the following equation [32]:

$$F = \frac{M}{l}(1 + \sin\varphi) \tag{1}$$

where F is the bending force, l is the die opening, $l = R_D + R_P + t$, R_D is the radius of the die, R_P is the radius of the punch, t is the

Table 2 Relation between BF and material volume removal

Cases	Sheet volume (mm^3)	Reduction in volume compared to no MD (%)	Reduction in BF compared to no MD (%)
MD-243	7125	5	59
MD-433	7195.2	4.1	29
MD-33	7225	3.7	33
MD-14	7289.2	2.8	29.5
Without MD	7500	0	—

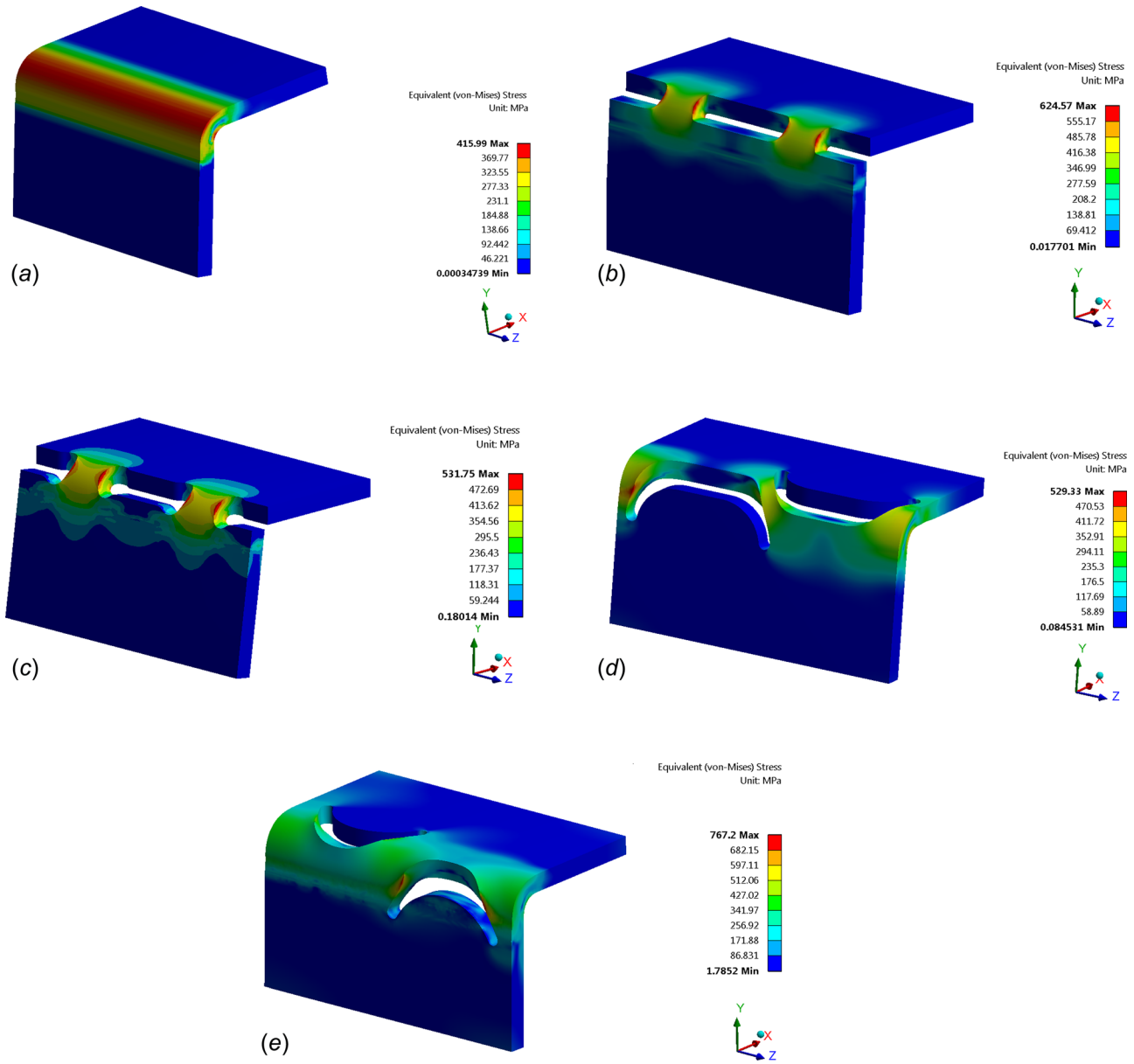

Fig. 8 Von Mises stress distribution for each MD case under study: (*a*) without MD, (*b*) MD-14, (*c*) MD-33, (*d*) MD-243, and (*e*) MD-433

thickness of the sheet, and ϕ is the bending angle, in this case it is equal to 90 deg, M is the bending moment, which is found using the following equation:

$$M = n(\text{UTS})\frac{bt^2}{4} \tag{2}$$

where n is correction coefficient hardening of a material ($n = 1.6$–1.8), UTS is the ultimate tensile strength of a material, b is width of the beam (length of bending) and t is the material thickness. Using Eq. (1), the bending force for the sheet without MD is found to be 15,210 (for $n = 1.8$), which is in good agreement with the bending force obtained from the FEA model, with a difference of 1.6%.

As for the evaluation of empirical bending force for the cases of MD, Eq. (1) cannot be used directly since the bending force is supposed to take into account the amount of material removed along the bending line. Hence, future investigation on the

Table 3 Maximum equivalent stresses

Cases	Max value (MPa)	Increase due to MD (%)
MD-243	529.3	27.2
MD-33	531.8	28
MD-14	624.6	50.1
MD-433	767.2	77.3
Without MD	416.0	—

mechanics of MD will be focused on developing general mathematical/empirical model for the calculation of bending force when MD exists on the bend line of a sheet.

Bending force reduction is related to the percentage of material removal in each MD case. In order to validate this hypotheses, volume of material removal in each MD case is tabulated in Table 2. It is noticed that the bending force reduction is not proportional to percentage of material volume removal. Implication of this hypotheses needs more rigorous studies.

Stress Evaluation

Von Mises stress is evaluated for all cases when the sheet is bent to 90 deg, as shown in Fig. 8. High stress is distributed along the bending line in all cases while the rest of the sheet body is subjected to less stress compared to the area along the bending line.

Von Mises stress values are higher when MD are present on a sheet. Based on the simulation results, with the effect of MD von Mises stress increased by 27.2% at minimum and by 77.3% at maximum case. Due to presence of MD, the stress distribution along the bend line is no longer uniform as in the case of the sheet without MD, see Table 3 and Fig. 8.

It is found that Von Mises stress in MD-33 decreased by 22.1% compared to MD-14. This is due to topological differences between MD-14 and MD-33. The enlarged circular openings in MD-33 helped transmit the stress into sheet body and thus it has less stress concentration. This indicates that the topological variation in MD can be utilized to reduce stress concentration depending on the design requirements of the sheet metal product.

Based on the results, MD-243 has overall best performance. The underlying reason is due to its profile—particularly, due to the fact that the profile of MD-243 has a larger radius of curvature along the bend line, which translates force easier compared to other MD profiles. The same can be said about MD-33. As for MD-433, the reason for it to be the highest in increase of stress is because of the edge-to-surface contact between edge of MD-433 pattern and surface of punch during bending. That is why maximum stress occurred on the edges of MD-433 pattern, see Fig. 8.

Springback

Spring back angle after bending is calculated for all cases. The results are tabulated in Table 4. It can be seen that application of MD reduced springback for all four MD cases. This conclusion validates similar results found in perforated sheet [33], where application of perforated feature at the bending area of sheet metal reduced springback. This implies potential of MD in reduction of springback.

Table 4 Springback angle after bending

Cases	Angle (deg)	Decrease due to MD (deg)
MD-243	92.666	0.375
MD-33	92.524	0.517
MD-14	92.439	0.603
MD-433	92.488	0.553
Without MD	93.041	—

Conclusion

Origami-based sheet metal is a new fabrication technique to produce sheet metal structures inspired by folding. The key element in this process is creating MD along the bend line that enables folding with reduction in the required bending force compared to the traditional sheet metal bending.

The shape and geometry of MD affect the required bending force, and, consequently, it is expected to reduce the manufacturing energy and cost associated with sheet metal fabrication. For the selected MD shapes, the required bending force was substantially reduced for all four cases in the FEA model. This reduction is caused by the material removal along the bend line leading to less material available to resist the bending force. The magnitude of reduction in bending force is associated with the percentage of volume removal. However, this relation between the percentage of material removal and resulting bending force is not proportional. Future work will focus on defining the exact relationship between the MD profile and the resulting bending force. Due to the small dimensions of MD, high stress concentration is generated along the bend line. On the other hand, the stress concentration can be effectively reduced with topological variation of MD and by introducing changes to the MD's profile. In addition, the application of MD leads to decrease in springback effect.

Funding Data

- Hellman Foundation (Hellman Faculty Fel).

Nomenclature

b = sheet width
F = bending force
g = clearance
l = die opening
M = bending moment
n = correction coefficient hardening of material
R_D = radius of die
R_P = radius of punch
t = sheet thickness
ϕ = bending angle

References

[1] Tekiner, Z., 2004, "An Experimental Study on the Examination of Springback of Sheet Metals With Several Thicknesses and Properties in Bending Dies," J. Mater. Process. Technol., **145**(1), pp. 109–117.

[2] Moon, Y. H., Kang, S. S., Cho, J. R., and Kim, T. G., 2003, "Effect of Tool Temperature on the Reduction of the Springback of Aluminum Sheets," J. Mater. Process. Technol., **132**(1–3), pp. 365–368.

[3] Ankenas, R., and Barauskas, R., 2006, "Finite Element Investigation on Parameters Influencing the Springback During Sheet Metal Forming," Mechanika, **5**(5), pp. 57–62.

[4] Banabic, D., 2010, *Sheet Metal Forming Processes: Constitutive Modelling and Numerical Simulation*, Springer Science and Business Media, Berlin, p. 6.

[5] Qattawi, A., Venhovens, P. J., and Brooks, J., 2014, "Rethinking Automotive Engineering Education—Deep Orange as a Collaborative Innovation Framework for Project-Based Learning Incorporating Real-World Case Studies," 121st ASEE Annual Conference and Exposition, Indianapolis, IN, June 15–18, pp. 1–28.

[6] Qattawi, A., Mayyas, A., Thiruvengadam, H., Kumar, V., Dongri, S., and Omar, M., 2014, "Design Considerations of Flat Patterns Analysis Techniques When Applied for Folding 3D Sheet Metal Geometries," J. Intell. Manuf., **25**(1), pp. 109–128.

[7] Qattawi, A., 2012, "Extending Origami Technique to Fold Forming of Sheet Metal," Ph.D. dissertation, Clemson University, Clemson, SC.

[8] Tachi, T., 2009, "Generalization of Rigid Foldable Quadrilateral Mesh Origami," International Association for Shell and Spatial Structures Symposium (IASS), Valencia, Spain, Sept. 28–Oct. 2, pp. 173–179.

[9] Tachi, T., 2011, "Rigid-Foldable Thick Origami," Fifth International Meeting of Origami Science, Mathematics, and Education (Origami 5), Singapore, July 13–17, pp. 253–264.

[10] Wu, W., and You, Z., 2011, "A Solution for Folding Rigid Tall Shopping Bags," Proc. R. Soc. London A, **467**(2133), pp. 2561–2574.

[11] Morgan, J., Magleby, S. P., and Howell, L. L., 2016, "An Approach to Designing Origami-Adapted Aerospace Mechanisms," ASME J. Mech. Des., **138**(5), p. 52301.

[12] Qattawi, A., Abdelhamid, M., Mayyas, A., and Omar, M., 2014, "Design Analysis for Origami-Based Folded Sheet Metal Parts," SAE Int. J. Mater. Manf., **7**(2), pp. 488–498.
[13] Venhovens, P., and Bell, K., 2013, "Application of a Novel Metal Folding Technology for Automotive BiW Design," SAE Int. J. Passeng. Cars-Mech. Syst., **6**(2), pp. 584–600.
[14] Gitlin, B., Kveton, A., and Lalvani, J., 2002, "Method of Bending Sheet Metal to Form Three-Dimensional Structures," Milgo Industrial Inc., Brooklyn, NY, U.S. Patent No. US 6,640,605 B2.
[15] Durney, M. W., and Pendley, A. D., 2013, "Precision-Folded, High Strength, Fatigue-Resistant Structures and Sheet Therefor," Industrial Origami LLC, Middleburg Heights, OH, U.S. Patent No. US 8,377,566 B2.
[16] Sullivan, J., Burnham, A., and Wang, M., 2010, *Energy-Consumption and Carbon-Emission Analysis of Vehicle and Component Manufacturing*, Argonne National Laboratory, Argonne, IL.
[17] Ablat, M. A., and Qattawi, A., 2016, "Finite Element Analysis of Origami-Based Sheet Metal Folding Process," ASME Paper No. IMECE2016-67324.
[18] Wifi, A., 1976, "An Incremental Complete Solution of the Stretch-Forming and Deep-Drawing of a Circular Blank Using a Hemispherical Punch," Int. J. Mech. Sci., **18**(1), pp. 23–31.
[19] Gotoh, M., and Ishisé, F., 1978, "A Finite Element Analysis of Rigid-Plastic Deformation of the Flange in a Deep-Drawing Process Based on a Fourth-Degree Yield Function," Int. J. Mech. Sci., **20**(7), pp. 423–435.
[20] Wang, N.-M., and Budiansky, B., 1978, "Analysis of Sheet Metal Stamping by a Finite-Element Method," ASME J. Appl. Mech., **45**(1), pp. 73–82.
[21] Banabic, D., 2010, *Sheet Metal Forming Processes: Constitutive Modelling and Numerical Simulation*, Springer Science and Business Media, Berlin, pp. 21–24
[22] Makinouchi, A., 1996, "Sheet Metal Forming Simulation in Industry," J. Mater. Process. Technol., **60**(1–4), pp. 19–26.
[23] Tekkaya, A. E., 2000, "State-of-the-Art of Simulation of Sheet Metal Forming," J. Mater. Process. Technol., **103**(1), pp. 14–22.
[24] Wenner, M. L., 2005, "Overview—Simulation of Sheet Metal Forming," AIP Conf. Proc., **778**(1), pp. 3–7.
[25] Lee, M. G., Kim, C., Pavlina, E. J., and Barlat, F., 2011, "Advances in Sheet Forming—Materials Modeling, Numerical Simulation, and Press Technologies," ASME J. Manuf. Sci. Eng., **133**(6), p. 061001.
[26] Reddy, P., Reddy, G., and Prasad, P., 2012, "A Review on Finite Element Simulations in Metal Forming," Int. J. Mod. Eng. Res., **2**(4), pp. 2326–2330.
[27] Makinouchi, A., Teodosiu, C., and Nakagawa, T., 1998, "Advance in FEM Simulation and Its Related Technologies in Sheet Metal Forming," CIRP Ann.—Manuf. Technol., **47**(2), pp. 641–649.
[28] Ablat, M. A., and Qattawi, A., 2016, "Numerical Simulation of Sheet Metal Forming: A Review," Int. J. Adv. Manuf. Technol., **89**(1–4), pp. 1235–1250.
[29] Oniate, E., Rojek, J., and Garino, C. G., 1995, "NUMISTAMP: A Research Project for Assessment of Finite-Element Models for Stamping Processes," J. Mater. Process. Technol., **50**(1–4), pp. 17–38.
[30] Yang, D. Y., Jung, D. W., Song, I. S., Yoo, D. J., and Lee, J. H., 1995, "Comparative Investigation Into Implicit, Explicit, and Iterative Implicit/Explicit Schemes for the Simulation of Sheet-Metal Forming Processes," J. Mater. Process. Technol., **50**(1–4), pp. 39–53.
[31] Wagoner, R., and Li, M., 2007, "Simulation of Springback: Through-Thickness Integration," Int. J. Plast., **23**(3), pp. 345–360.
[32] Boljanovic, V., 2004, *Sheet Metal Forming Processes and Die Design*, Industrial Press, New York, pp. 50–52.
[33] Nasrollahi, V., and Arezoo, B., 2012, "Prediction of Springback in Sheet Metal Components With Holes on the Bending Area, Using Experiments, Finite Element and Neural Networks," Mater. Des., **36**, pp. 331–336.